

# ON THE ORIGIN OF THE SUPERGIANT HI SHELL AND PUTATIVE COMPANION IN NGC 6822

JOHN M. CANNON<sup>1</sup>, ERIN M. O’LEARY<sup>1</sup>, DANIEL R. WEISZ<sup>2</sup>, EVAN D. SKILLMAN<sup>3</sup>, ANDREW E. DOLPHIN<sup>4</sup>, FRANK BIGIEL<sup>5</sup>,  
ANDREW A. COLE<sup>6</sup>, W.J.G. DE BLOK<sup>7</sup>, FABIAN WALTER<sup>8</sup>,

<sup>1</sup>Department of Physics & Astronomy, Macalester College, 1600 Grand Avenue, Saint Paul, MN 55105; jcannon@macalester.edu

<sup>2</sup>Department of Astronomy, University of Washington, Seattle, WA 98195

<sup>3</sup>Minnesota Institute for Astrophysics, University of Minnesota, Minneapolis, MN 55455, USA

<sup>4</sup>Raytheon Company, 1151 East Hermans Road, Tucson, AZ 85706

<sup>5</sup>Institut für Theoretische Astrophysik, Universität Heidelberg, Albert-Ueberle-Str. 2, 69120 Heidelberg, Germany

<sup>6</sup>University of Tasmania, School of Mathematics & Physics, Private Bag 37, Hobart, Tasmania 7001

<sup>7</sup>Department of Astronomy, University of Cape Town, Rondebosch 7700, South Africa

<sup>8</sup>Max-Planck-Institut für Astronomie, Königstuhl 17, D-69117, Heidelberg, Germany

*Accepted for Publication in the Astrophysical Journal*

## ABSTRACT

We present new *Hubble Space Telescope* Advanced Camera for Surveys imaging of six positions spanning 5.8 kpc of the HI major axis of the Local Group dIrr NGC 6822, including both the putative companion galaxy and the large HI hole. The resulting deep color magnitude diagrams show that NGC 6822 has formed >50% of its stars in the last ~5 Gyr. The star formation histories of all six positions are similar over the most recent 500 Myr, including low-level star formation throughout this interval and a weak increase in star formation rate during the most recent 50 Myr. Stellar feedback can create the giant HI hole, assuming that the lifetime of the structure is longer than 500 Myr; such long-lived structures have now been observed in multiple systems and may be the norm in galaxies with solid-body rotation. The old stellar populations (red giants and red clump stars) of the putative companion are consistent with those of the extended halo of NGC 6822; this argues against the interpretation of this structure as a bona fide interacting companion galaxy and against its being linked to the formation of the HI hole via an interaction. Since there is no evidence in the stellar population of a companion galaxy, the most likely explanation of the extended HI structure in NGC 6822 is a warped disk inclined to the line of sight.

*Subject headings:* galaxies: evolution — galaxies: dwarf — galaxies: irregular — galaxies: individual (NGC 6822)

## 1. INTRODUCTION

Holes and shells in the neutral interstellar medium of star-forming galaxies have been challenging to interpret for decades. While alternative creation mechanisms exist, and the details of the energetics and multi-phase interactions are very complex (see, e.g., discussion in Tenorio-Tagle & Bodenheimer 1988), recent results support a scenario where energetic processes associated with stellar evolution (feedback) are the primary mechanism by which such structures are created (a very short and incomplete list would include Weisz et al. 2009a, Weisz et al. 2009b, Cannon et al. 2011a, Cannon et al. 2011b, Warren et al. 2011, and the numerous references therein). Many of these results have been attained in low-mass dwarf galaxies, where the lack of large-scale dynamical processes (i.e., spiral density waves) allows the characteristic timescale of the gas structures to extend for long periods of time (longer than a few hundred Myr in the aforementioned studies). The stellar feedback cycle can be considered one of the primary internal catalysts of galaxy evolution.

A second driver of rapid galaxy evolution is gravitational interactions with companion systems. Interactions between massive galaxies can cause powerful starburst episodes (e.g., Heckman et al. 1990); similarly, interactions between dwarf and massive galaxies can be dramatic (e.g., the Magellanic Stream being pulled from the SMC/LMC system by interactions with the Milky Way; Putman et al. 1998). However, interactions between low-

mass systems, which were frequent in the early universe, are less common at low redshift. Part of the reason is that most present day star forming, gas-rich dwarf galaxies are found in regions of comparative isolation or in loose associations such as the Local Group. Thus, “isolated” dwarf galaxies (i.e., not satellites of massive systems) that are undergoing interactions with other low-mass objects are rare, with only a few well-studied examples (e.g., VCC 848 - Gallagher & Hunter 1989). Interactions between companion low-mass systems is a relatively unexplored driver of dwarf galaxy evolution.

At a distance of  $492 \pm 20$  kpc ( $1'' = 2.4$  pc; Lee et al. 1993; Dolphin et al. in preparation), NGC 6822 is among the nearest star forming dIrrs in the Local Group. This system is gas-rich, dark-matter dominated (de Blok & Walter 2000), and resembles the SMC in size and luminosity ( $M_B \sim -15.8$ ; Hodge et al. 1991). It is not associated with the concentrations of galaxies surrounding M31 or with the Milky Way (Mateo 1998). While the system is well-studied (more than 600 journal references to date), and is in our cosmological backyard, the internal and external processes that drive its evolution remain poorly constrained.

NGC 6822 provides an opportunity to study a system that is currently being shaped by both internal (stellar feedback) and external (low-mass gravitational interaction) processes. The neutral gas disk is dominated by an intricate structure of holes and shells (see Figure 1, and de Blok & Walter 2000, 2006). The most impres-

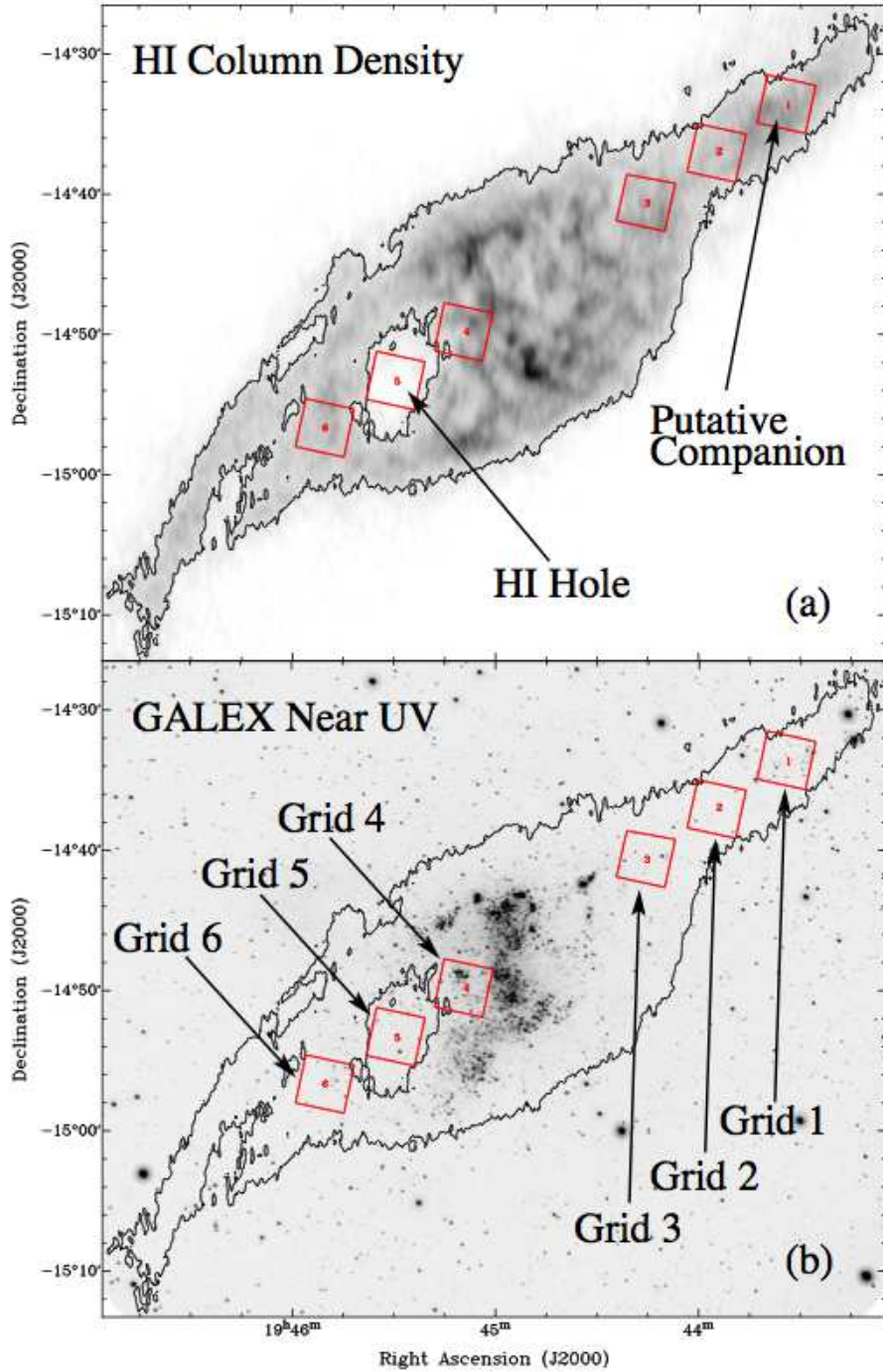


FIG. 1.— HI column density image (a; see de Blok & Walter 2000) and archival GALEX image (b) of NGC 6822, with the six observed grid positions overlaid in red and labeled from “1” (northwest) to “6” (southeast). Grid 1 contains the putative companion and grid 5 is located within the HI hole. The black contour highlights the HI column density at the  $5 \times 10^{20} \text{ cm}^{-2}$  level.

sive feature is a large hole spanning some  $2 \text{ kpc} \times 1.4 \text{ kpc}$  (labeled “HI Hole” in Figure 1); this is one of the largest known holes in the ISM of a nearby dwarf galaxy. Equally remarkable is the presence of a putative small companion galaxy ( $M_{\text{HI}} \sim 10^7 M_{\odot}$ ) that appears to be interacting with the main disk (labeled “Putative Companion” in Figure 1). de Blok & Walter (2000) demonstrate a significant offset in velocity between this northwest HI cloud and NGC 6822, arguing for the object being a physically separate low-mass system (see further

discussion below). NGC 6822 is thus exceptional in that it has both a giant HI hole and a putative low-mass companion in close proximity; it is one of the only known galaxies with both properties.

The ground-based optical study by de Blok & Walter (2006) used deep *Subaru* data covering the entire HI disk to resolve the bright O and B stars in NGC 6822. That study revealed the surprising presence of numerous young stars (ages  $< 10^8 \text{ yr}$ ) throughout the entire HI disk, well beyond  $R_{25}$ . Young blue stars were found associated

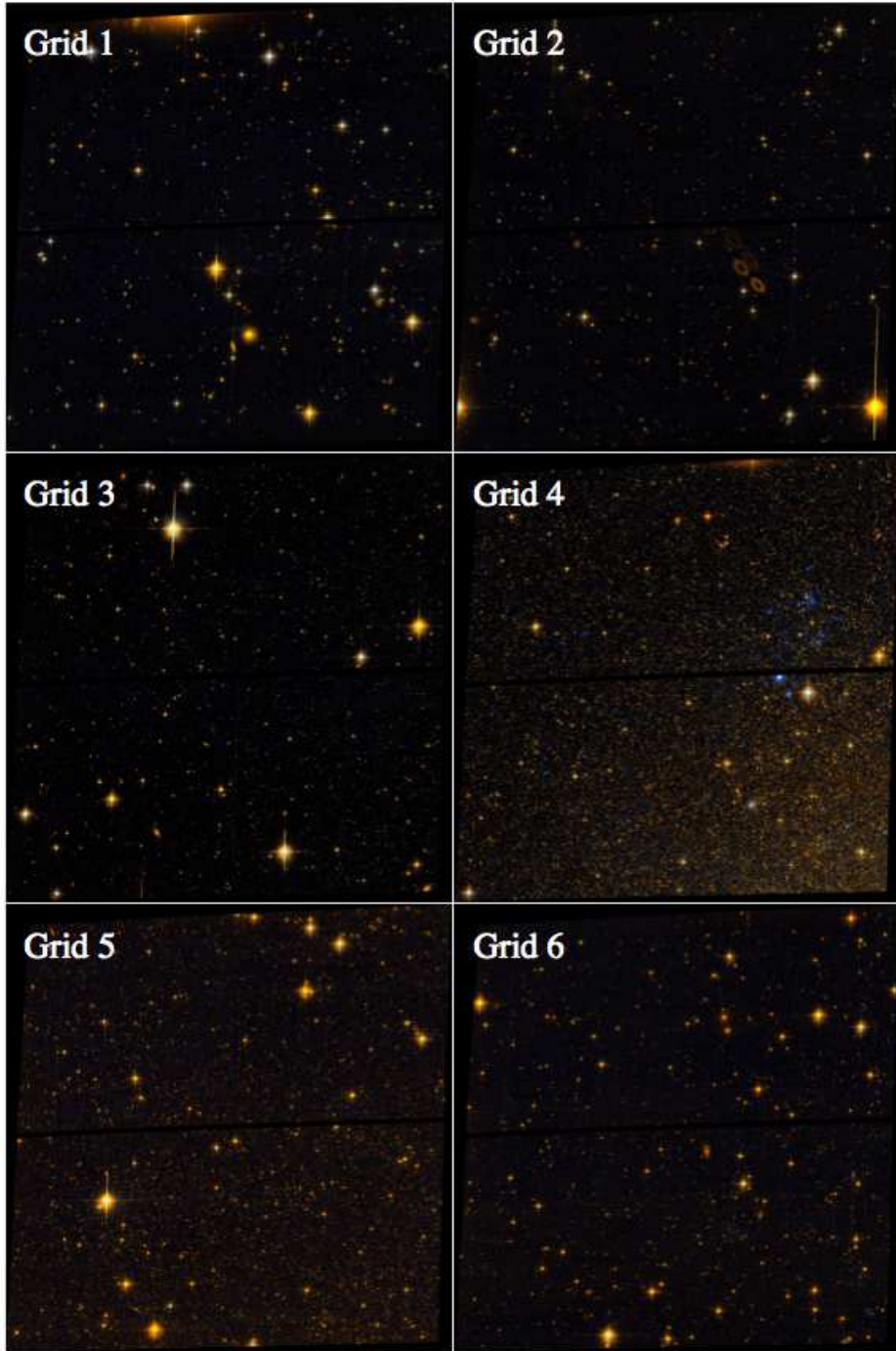


FIG. 2.— Two-color images of the six grid fields; each image is the size of the ACS field of view ( $202'' \times 202''$ ) and is shown in an un-rotated orientation. While the stellar density varies considerably from grid to grid, there are blue stars clearly detected in all locations probed by these images.

with the putative companion galaxy, indicating that star formation (SF) has been ongoing there for at least the last  $10^8$  yr (see de Blok & Walter 2006). Further, there are also relatively young stars located in the outer HI disk.

The goal of the present investigation is to study the underlying stellar populations in the giant HI hole and in the putative companion, thus probing both the internal and external processes that are driving the recent evolution of NGC 6822. New *Hubble Space Telescope* (HST)

Advanced Camera for Surveys (ACS; Ford et al. 1998) imaging is acquired in six positions along the HI major axis. Each position is labeled in Figure 1, from “grid 1” through “grid 6”, moving from NW to SE; note that the grid 1 position is coincident with the putative companion, while the grid 5 position is coincident with the HI hole. The extracted resolved stellar photometry reaches well below the red clump, allowing an accurate measurement of the global SFH as well as the recent SFH (with high time resolution over the past  $\sim 500$  Myr). The SFHs

TABLE 1  
HST OBSERVATIONS OF NGC 6822

Grid	RA	DEC	F475W $t_{\text{int}}$	F814W $t_{\text{int}}$	# of Matched	F475W 50% Completeness	F814W 50% Completeness
#	(J2000)	(J2000)	(sec)	(sec)	Stars	(mag)	(mag)
1	19 <sup>h</sup> 43 <sup>m</sup> 33.50 <sup>s</sup>	−14°33′41.0 <sup>s</sup>	886	1346	4715	26.8	25.5
2	19 <sup>h</sup> 43 <sup>m</sup> 54.02 <sup>s</sup>	−14°37′09.6 <sup>s</sup>	1119	1118	5824	26.8	25.5
3	19 <sup>h</sup> 44 <sup>m</sup> 14.87 <sup>s</sup>	−14°40′39.7 <sup>s</sup>	1119	1118	15850	26.8	25.5
4	19 <sup>h</sup> 45 <sup>m</sup> 10.25 <sup>s</sup>	−14°49′46.4 <sup>s</sup>	1119	1118	195588	26.2	24.9
5	19 <sup>h</sup> 45 <sup>m</sup> 30.26 <sup>s</sup>	−14°53′14.3 <sup>s</sup>	1119	1118	52449	26.6	25.3
6	19 <sup>h</sup> 45 <sup>m</sup> 51.13 <sup>s</sup>	−14°56′36.7 <sup>s</sup>	886	1346	13435	26.8	25.4

we derive provide strong temporal constraints on the creation of the various structures observed in the optical and in HI. This is a unique opportunity to study multiple important evolutionary processes in dwarf galaxies.

## 2. OBSERVATIONS AND DATA REDUCTION

Six positions spanning the HI major axis of NGC 6822 were observed for one orbit each in Cycle 18 for program GO-12180 (P.I. Cannon); these six positions, labeled as grid 1 through grid 6, are shown by red boxes in Figure 1. The *HST*/ACS was used to acquire images in the F475W and F814W filters in two visits (grids 1, 2, and 3 observed on October 22, 2010; grids 4, 5, and 6 observed on March 28-29, 2011). Two images were acquired with each filter at each position, with integration times differing slightly between grids (886 and 1346 seconds for F475W and F814 in grids 1 and 6, and 1119 and 1118 seconds for F475W and F814 in grids 2, 3, 4 and 5). No dithering strategy was applied; each filter’s observation was CRSPLIT into two images to facilitate the removal of cosmic rays. Hot pixels are easily differentiated from stars using our photometric measurement tools (see below). Figure 2 shows color representations of each *HST* field of view; the presence of both young blue stars and a diffuse red stellar population is obvious in all grid positions.

We performed stellar PSF photometry using the DOLPHOT software package, a modified version of HSTPHOT (Dolphin 2000) with an ACS specific module. To separate well-measured stellar sources from artifacts, we applied quality criteria to the raw photometric catalogs in each field. Specifically, a well-measured star satisfied the following criteria:  $\text{SNR}_{\text{F475W}} > 5.0$  and  $\text{SNR}_{\text{F814W}} > 5.0$ ,  $(\text{sharp}_{\text{F475W}} + \text{sharp}_{\text{F814W}})^2 < 0.075$ , and  $(\text{crowd}_{\text{F475W}} + \text{crowd}_{\text{F814W}}) < 1.0$ . The 50% completeness levels and numbers of matched stars in each grid location are given in Table 1. To characterize the observational uncertainties and completeness functions, in each field we performed 500,000 artificial star tests. In order to compute the completeness function, the artificial star tests were culled using identical criteria to the photometry. The results of these tests are shown in Figure 3, which plots the photometric completeness as a function of magnitude for each of the six grid positions. The photometric depths and completeness functions are nearly identical for all six grid positions.

Figure 4 presents the color magnitude diagram (CMD) of each grid position using a density contour approach (i.e., a “Hess diagram”). Our photometry is complete well below the red clump and fully samples the blue he-

lium burning (BHeB) region of the CMD in each grid (see Weisz et al. 2008 for a complete discussion of these various CMD regions). Note the differences in stellar density from one grid to the next (e.g., grid 4 contains  $\sim 40$  times more matched stars than grid 1).

An accurate CMD of a galaxy’s stellar populations allows the derivation of the intensity of SF as a function of both time and of location, i.e., a star formation history (SFH). To derive the SFH, we apply a maximum-likelihood technique that fits the observed features of the CMD with a set of synthetic CMDs. The SFH of the best fitting synthetic CMD is the most probable SFH of the observed stellar population. We refer the reader to Dolphin (2002), Dolphin et al. (2003), and Dolphin (2012, in preparation) for detailed discussion and demonstrations of this technique and its ability to differentiate flat SFHs from those with temporal features.

The synthetic CMDs are a linear combination of simple stellar populations that have been convolved with observational biases as determined by artificial star tests. We generate each synthetic population by assuming a stellar initial mass function and a binary star fraction, and designating a number and resolution of bins in both age and metallicity. Further, the observed and synthetic CMDs are binned to facilitate statistical comparisons between the two.

In the case of NGC 6822, we have adopted a Kroupa IMF (Kroupa 2001) within a mass range of 0.15 to 120  $M_{\odot}$ , a binary fraction of 0.35, and the Padova stellar evolution models (Girardi et al. 2002 and Girardi et al. 2010). To balance computational efficiency with the desire for a detailed SFH, we selected 36 time bins with uniform logarithmic spacing between  $\log(t) = 6.6$  and 10.15 and an isochronal metallicity range from 0.0001  $Z_{\odot}$  to 0.0019  $Z_{\odot}$  with a resolution of 0.1 dex. The data do not contain significant main sequence turn off features for populations older than  $\sim 5$  Gyr, and we thus have only poor constraints on the lifetime chemical evolution. Therefore, we required that the metallicities monotonically increase to minimize potential non-physical chemical models resulting from the RGB age-metallicity degeneracies (e.g., Gallart et al. 2005). We have designated the 50% completeness limits as the faintest photometric depths considered.

Intervening Milky Way foreground stars can contaminate the observed CMD. To mitigate this effect, we have included a model foreground CMD in the SFH measurements. This CMD was constructed with the Dartmouth isochrones (Dotter et al. 2008), which extend to slightly lower masses of 0.1  $M_{\odot}$ , and follow the color and magni-

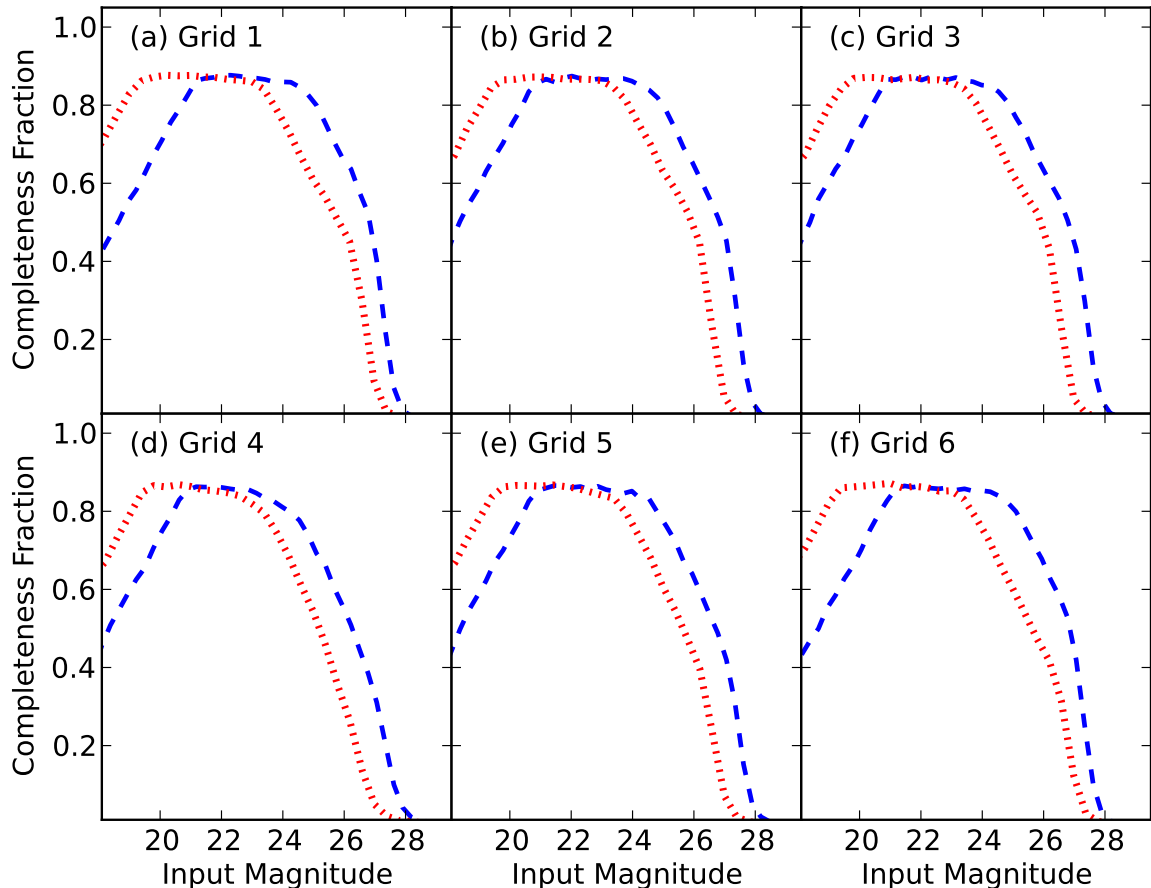


FIG. 3.— Photometric completeness as a function of magnitude for each of the six grid positions. The blue and red lines represent the functions for the F475W and F814W filters, respectively. The photometric depths and completeness functions are nearly identical for all six grid positions.

tude distributions detailed in de Jong et al. (2010). Finally, given the relative sparseness of the TRGB populations in each field, we fixed the distance to previous TRGB determinations (see § 1). However, we allowed the code to solve for the optimal extinction value to each field, as NGC 6822 appears to have significant variations in extinction from field to field.

In this study, we are interested in comparing the SFHs derived for each grid position; each of the six CMDs contains data of comparable photometric depths and similar error functions (see Figure 3). The similarity of data quality at each position means that the uncertainties on the SFHs reflect the observational errors and the random uncertainties due to the number of stars. The random uncertainties are calculated by performing 50 Monte Carlo tests that use a Poisson random noise generator to create a random sampling of the best-fit CMD. We do not consider the systematic uncertainties introduced by choice of stellar evolution models that are typically calculated in SFH derivations; in the limit of comparable quality data these choices do not affect the differential measurements from one position to another (e.g., Weisz et al. 2011).

### 3. STAR FORMATION HISTORIES IN THE SIX GRID POSITIONS

The cumulative SFHs of all six grid positions are presented in Figure 5. This shows, for lookback times beginning at the Big Bang and decreasing until the present

day, the fraction of the total stellar mass in each field that formed at or before a given time. All grid positions are normalized to a cumulative value of unity at the present day. When a given region reaches a cumulative SF of 0.5, then 50% of the total stellar mass in that region has formed; we hereafter refer to this timescale, measured back from the present day, as  $\tau_{50}$ . The solid lines represent the best-fit cumulative SFH for each grid; the dotted lines represent the  $1\sigma$  error bounds (technically the bounds at the 16<sup>th</sup> and 84<sup>th</sup> percentiles) derived from Monte Carlo simulations.

While some variations exist, the cumulative SFHs of the six grid positions are qualitatively consistent with one another from the Hubble time up until  $\sim 6$  Gyr ago. This is strong evidence for the entire NGC 6822 system evolving as a single entity during this period. If the putative companion in grid 1 were in fact undergoing its first episode of SF at the present time, then such a signature would be very obvious in the plot as a long period of quiescence followed by a rapid increase in the cumulative SF in recent epochs. No such pattern is seen for the stars detected in grid 1. We note that our age resolution is most coarse for these ancient bins; however, this caveat strengthens our interpretation. Even if the details of the ancient SFH are less certain than those at recent times, Figure 5 shows that the field containing the putative companion has formed the highest fraction of its stars at old ages compared to the other fields. In fact,



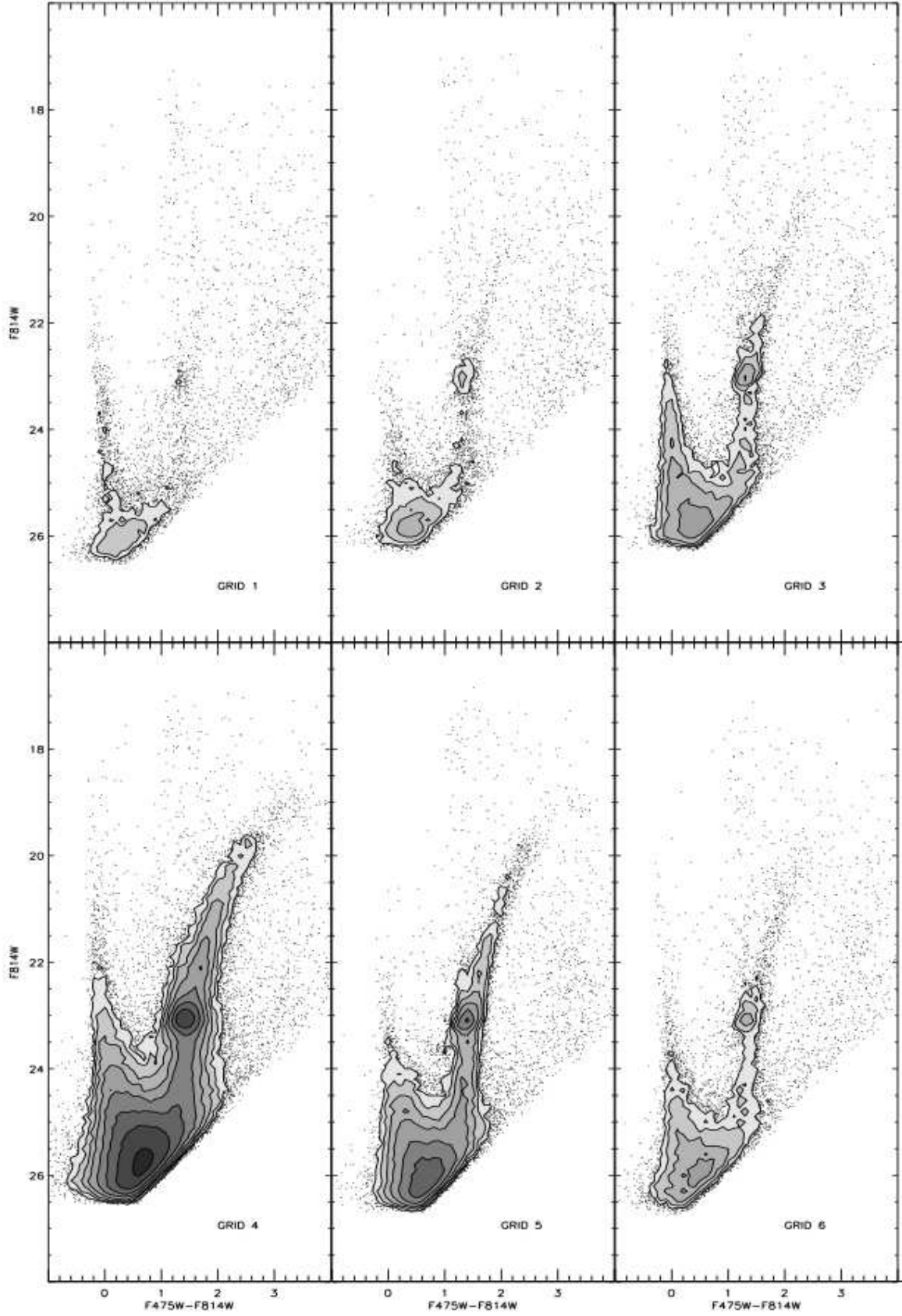


FIG. 4.— Hess diagram CMDs of each grid, as labeled; each grid is corrected for MW foreground extinction via the best-fit value from SFH analysis. Contours are at the same levels (10, 20, 40, 80, 160, 320, 640, 1280, 2560 stars  $\text{decimag}^{-2}$ ) in all panels.

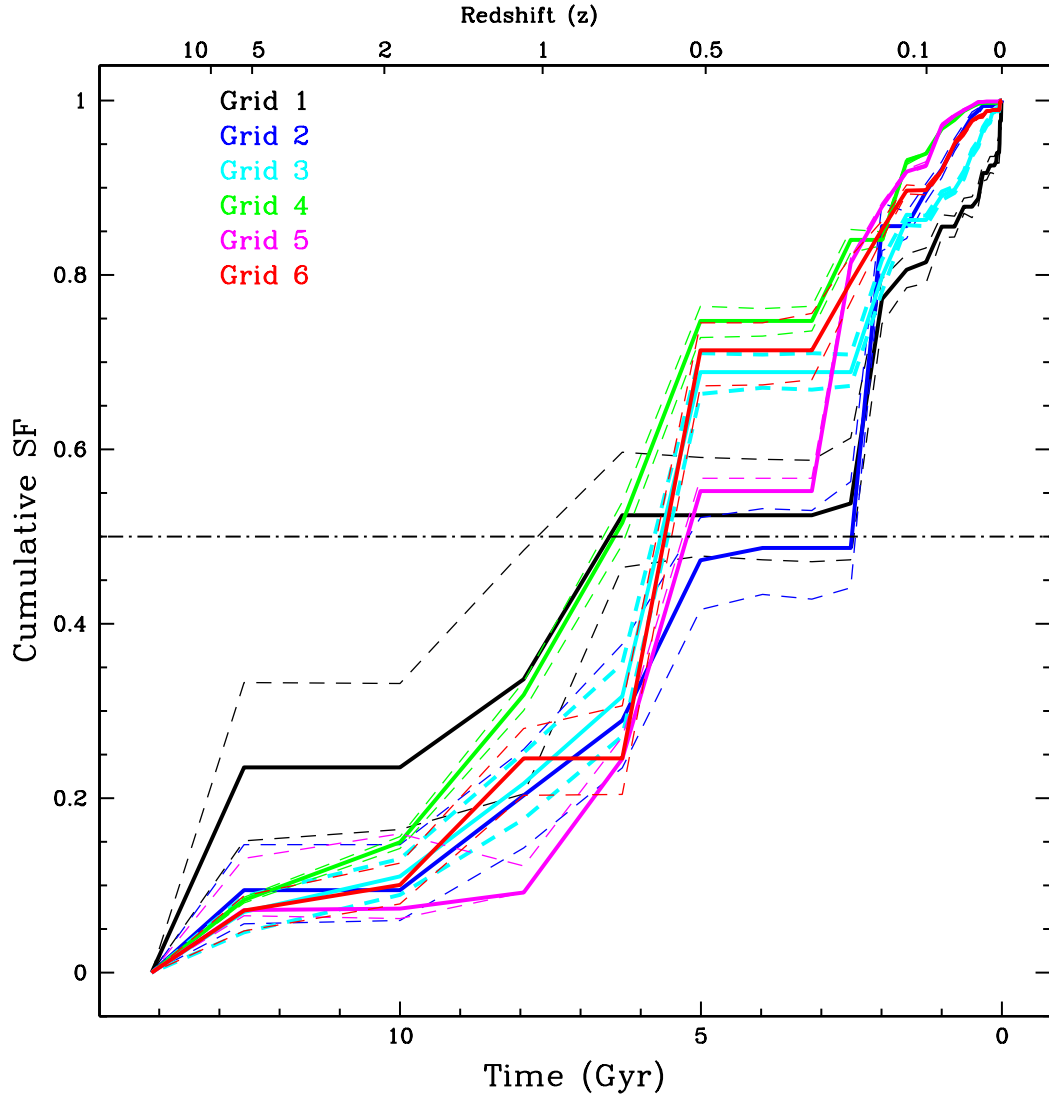


FIG. 5.— The cumulative SFHs of each grid. The solid lines represent the best-fit cumulative SFH for each grid; the dotted lines represent the  $1\sigma$  error bounds (technically the bounds at the 16<sup>th</sup> and 84<sup>th</sup> percentiles) derived from Monte Carlo simulations. When a given region reaches a cumulative SF of 0.5, then 50% of the total stellar mass in that region has formed. These plots demonstrate that NGC 6822 has formed  $\sim 50\%$  of its stellar mass within the most recent 5 Gyr. The redshifts at the top of the plot were computed assuming a WMAP7 cosmology (Jarosik et al. 2011).

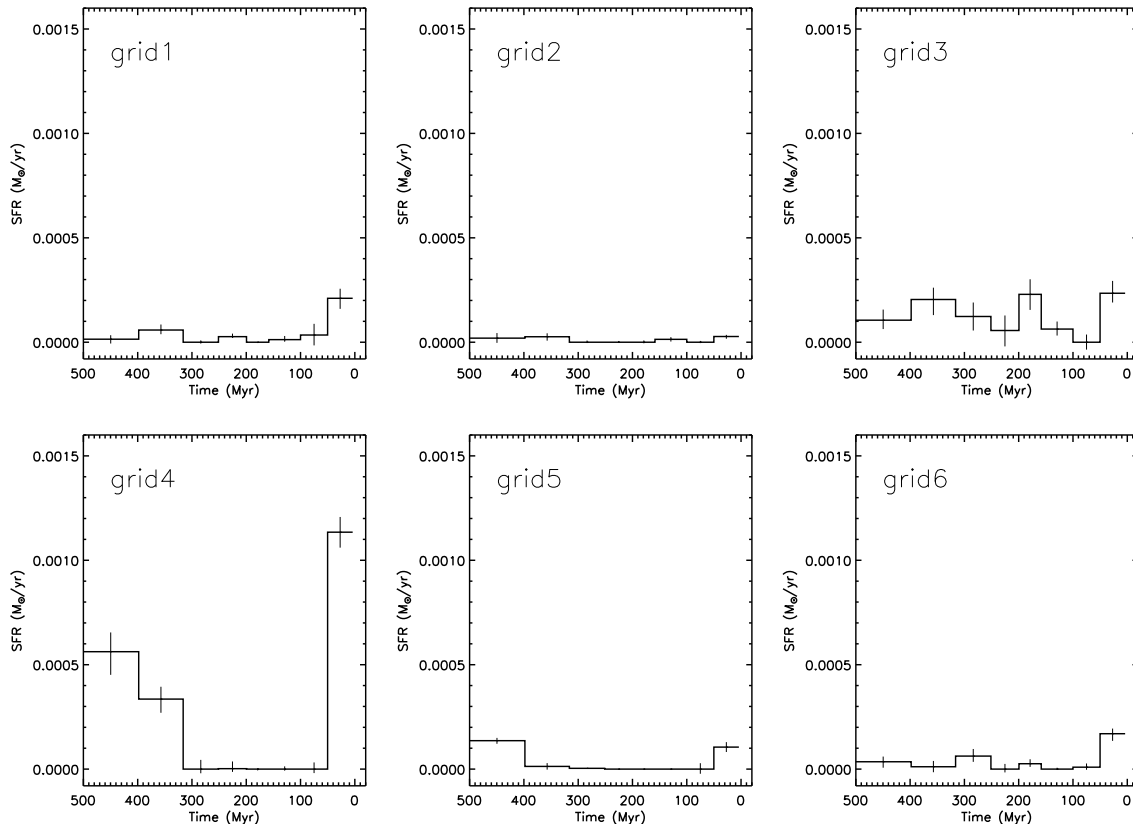


FIG. 6.— Recent SFHs in each grid over the most recent 500 Myr; note that time increases from 0 Myr (present day) to 500 Myr leftward on the abscissae. The general shapes of the SFHs are similar in all grids (i.e., the periods of relative activity are contemporaneous), although the strength of SF varies from one grid position to the next.

this is exactly what is expected if the outer field contains just the extended disk and not a companion. Numerous studies of the resolved stars of nearby dwarf galaxies have shown that the outer regions have higher fractions of older stars (e.g., Dohm-Palmer et al. 1997, 1998; Gallagher et al. 1998; Tolstoy et al. 1998). This nearly universal characteristic of dwarf galaxies has been interpreted as the result of the active star-forming region of the galaxy shrinking with time (Hidalgo et al. 2003), and has been supported by very detailed spatially resolved SFHs (e.g., Hidalgo et al. 2009).

As Figure 5 shows, NGC 6822 has formed roughly half of its stars within the most recent 5 Gyr (i.e.,  $\tau_{50} \simeq 5$  Gyr). This is broadly consistent with the value  $\tau_{50} = 6.9$  Gyr reported by Orban et al. (2008) in a reanalysis of archival *HST* images near the center of NGC 6822, who found that 57% of the lifetime star formation took place in the past 5 Gyr. Our derived  $\tau_{50}$  value can be compared with measurements of the same timescale for other nearby galaxies. Using a sample of seven Local Group dIrr galaxies, Weisz et al. (2011) calculates a characteristic timescale of  $\sim 6$  Gyr for the formation of 50% of the stellar mass; NGC 6822 thus is very similar to other Local Group dIrrs. Interestingly, the  $\tau_{50}$  level for 25 other dIrr galaxies from the Weisz et al. (2011) sample (mostly outside the Local Group) show an average  $\tau_{50}$  that is about a factor of two longer (i.e., a greater fraction of early star formation).

The more recent cumulative SFHs (from  $\sim 6$  Gyr to the present) do show some appreciable differences between

grids 1, 2, and 5 and the other three. Specifically, grids 1, 2, and 5 show a period of relative quiescence (i.e., little to no increase in the cumulative SF) between  $\sim 6$  and  $\sim 3$  Gyr, while grids 3, 4, and 6 show an increasing cumulative SF during the same interval. Around  $\sim 2$ -3 Gyr ago, grids 1, 2, and 5 show a significant increase in cumulative SF. This could be interpreted as weak evidence for an interaction involving the material now located in grids 1 and 2 with the material currently located in grid 5. More specifically, this could be interpreted as weak evidence for an interaction scenario leading to the creation of the large HI hole at the position of grid 5. We discuss this hypothesis in more detail below.

The overall similarity of the cumulative SFHs of the six NGC 6822 grids, especially in the epochs more ancient than  $\sim 6$  Gyr, can be interpreted as the lack of evidence for inside-out growth of its disk. Within the errors, the outermost field is as ancient as the inner fields. This contrasts with the results of Williams et al. (2009), who detect the signature of increasing disk scale length with cosmic time in M33. The cumulative SFH of NGC 6822 can be considered to be intermediate between the extreme Local Group dwarfs LGS-3 (which formed  $\sim 90\%$  of its stars in an intense SF event more than 11 Gyr ago; Hidalgo et al. 2011) and Leo A (which formed 90% of its stars more recently than 8 Gyr ago, with a peak in the most recent  $\sim 1.5$ -4 Gyr period; Cole et al. 2007).

The present study focuses on the recent patterns of star formation throughout NGC 6822. The recent SFHs (in  $M_{\odot} \text{ yr}^{-1}$ ) in each grid location as a function of time,



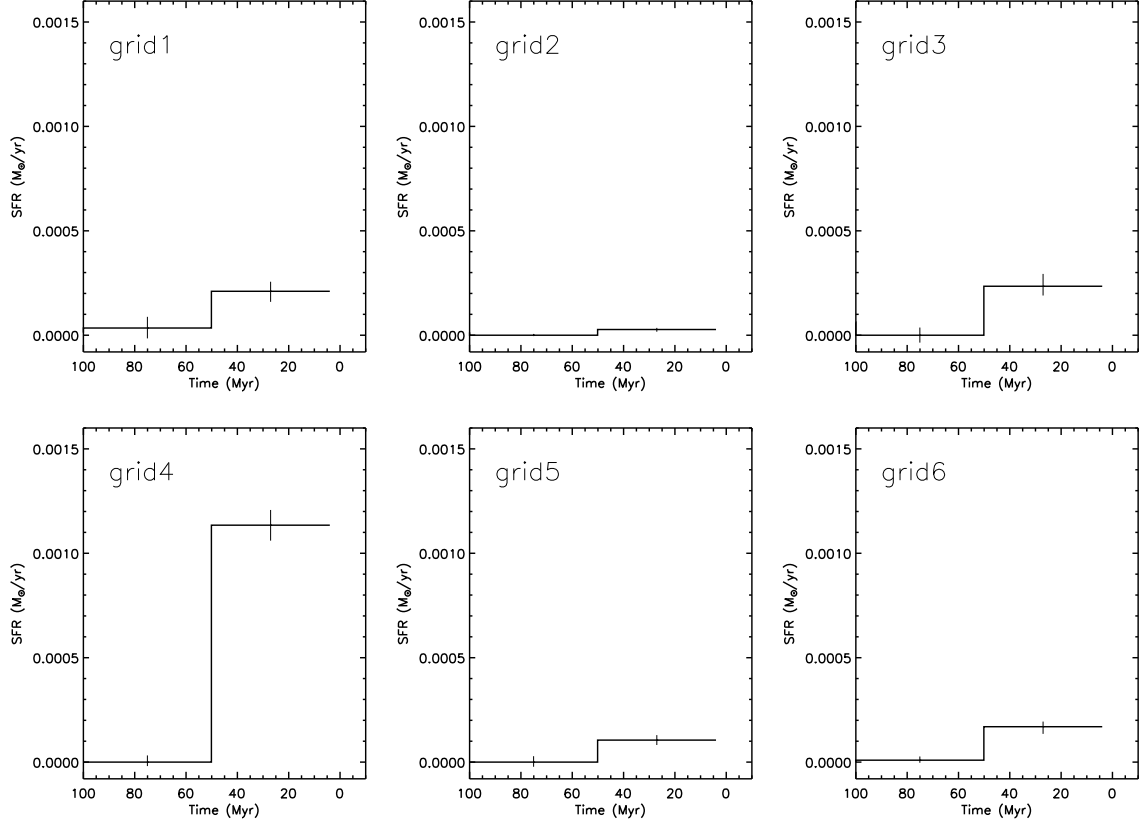


FIG. 7.— Recent SFHs in each grid over the most recent 100 Myr; note that time increases from 0 Myr (present day) to 100 Myr leftward on the abscissae.

over the last 500 Myr and 100 Myr, are presented in Figures 6 and 7, respectively. Note that since each panel presents the SFH derived from all stars in the entire ACS field of view at each grid location, the SFHs can also be considered in units of star formation rate (SFR) per unit time per unit area (the  $\sim 202'' \times 202''$  field of view of the ACS translates to  $\sim 482 \times \sim 482$  pc or  $\sim 0.23$  kpc<sup>2</sup> at the distance of 492 pc). From the longer-duration SFHs (Figure 6) it is clear that the SFR in each grid (with the exception of grid 4) has been essentially flat over the last 500 Myr; no major SF events are apparent in any grid location (except perhaps grid 4) until the most recent  $\sim 50$  Myr interval.

As Figure 7 shows, all six fields show evidence of an increased rate of star formation in the last 50 Myr (although with considerable differences in the amplitude of increase from one grid location to the next). Such a global increase in star formation, which is happening on a time scale which is short compared to the dynamical time scale ( $\sim 140$  Myr; McQuinn et al. 2010) is often associated with an interaction. Thus, we next investigate the possibility that the NW HI concentration is a companion galaxy.

#### 4. ON THE NATURE OF THE PUTATIVE COMPANION

The original interpretation of the NW region as a companion galaxy by de Blok & Walter (2000, 2003, 2006) was based on the observed neutral gas velocity offset (compared to the rest of the HI disk) in this region and on the presence of a significant number of spatially coincident young stars. de Blok & Walter (2006) derive a

total luminosity of  $M_B = -7.8$  for the stars in the NW cloud, and estimate a total stellar mass of  $\sim 10^5 M_\odot$ . This putative companion thus is very gas-rich ( $M_{\text{HI}}/L_B > 10$  depending on model assumptions).

The similarity of the ancient SFHs in all six grid positions discussed above appears to contradict the interpretation of this system as a companion galaxy. However, the more recent cumulative SF rates in each grid position show some weak characteristics that might be consistent with an interaction scenario. We now use the information on the stellar populations in the six grid positions to address the question: is the NW region a bona fide companion galaxy that is interacting with NGC 6822 at the present time?

Fundamental to our interpretation is the assumption that if this is a bona fide companion galaxy, then it should harbor an ancient stellar population. This assumption is based on the detection of such a population (i.e., red clump and red giant branch stars) in every galaxy for which adequate data exist, even extending to the most metal-poor (e.g., IZw 18; see Östlin 2000, Fiorentino et al. 2010, and the various references therein) or the most extreme SFH cases (e.g., Leo A, with the bulk of its SF delayed until the most recent few Gyr; see discussion above and in Cole et al. 2007).

If the putative companion of NGC 6822 is a bona fide dwarf galaxy, then our ACS images of grid 1 should reveal an over-density of old stars at this location. Further, the ground-based *Subaru* imaging of the outer regions of NGC 6822 by de Blok & Walter (2006) should verify this signature. We thus explore both datasets in an attempt

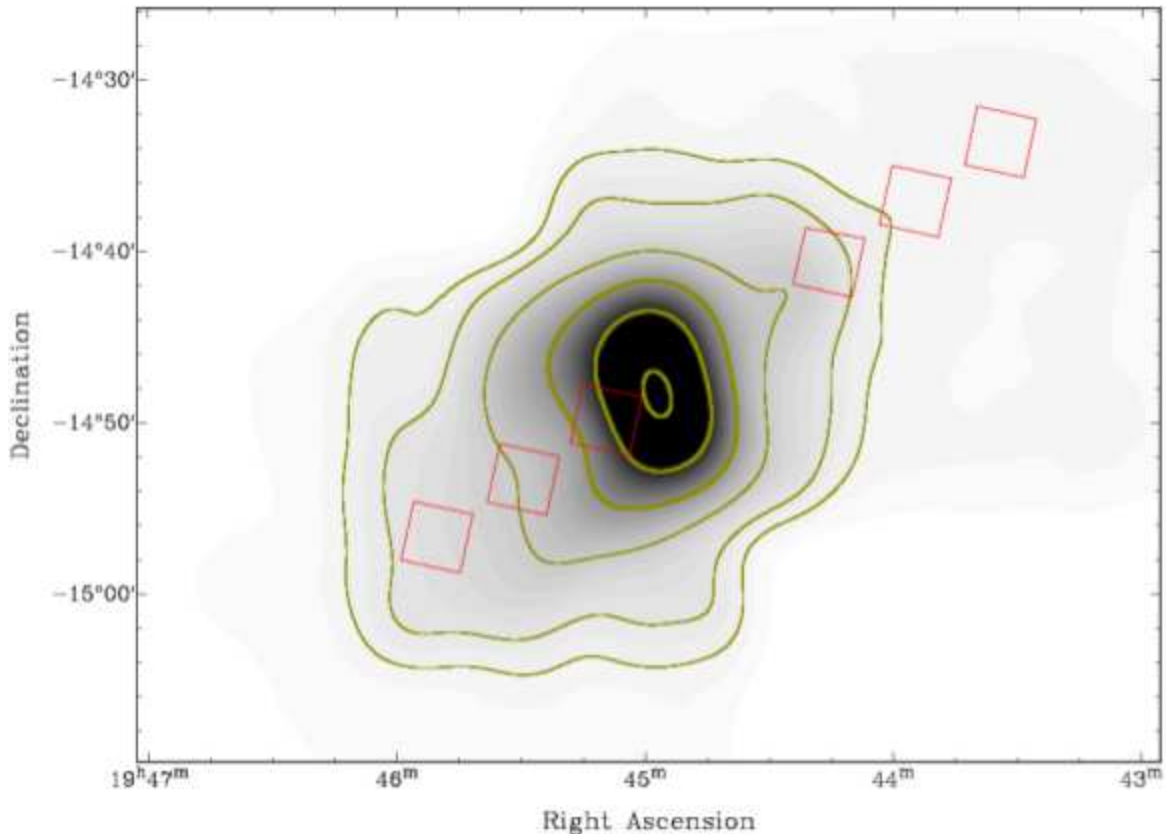


FIG. 8.— Smoothed distribution of red giant branch stars detected in the combined *Subaru* dataset from de Blok & Walter (2006). The six grid positions observed by *HST* are overlaid. In grid 1 we see no spatial concentration of red giant branch stars indicative of the companion.

to identify this ancient stellar over-density.

Figure 8 shows the spatial distribution of all red giant branch stars detected in the *Subaru* images; the locations of the six ACS grids are overlaid. While we are cognizant that crowding will be more severe in ground-based images compared to our new ACS images, the quality of the CMDs obtained by de Blok & Walter (2006) allow an unambiguous separation of the red giant branch component from the blue plume. This figure shows no evidence for a spatial concentration of red giant branch stars at the location of the putative companion.

A direct comparison of the ACS and *Subaru* images is challenging not only due to the differences in crowding but also due to the difference in photometric depth; *HST* will more easily detect a faint over-density of red stars. With these caveats in mind, Figure 9 shows the smoothed distributions of red giant branch stars detected by both *HST* and *Subaru* in the position of grid 1. We stress that a one-to-one agreement between these panels is not expected due to differences in crowding and depth. Again, the grid 1 position shows no obvious over-density of red giant branch stars indicative of a stellar companion.

It is conceivable that the ancient stellar population of the putative companion has a sufficiently low surface brightness that it is below the sensitivity of the *Subaru* data to detect. Further, it is conceivable that the ancient stars of this putative companion are distributed over an area larger than the projected size of the ACS field of view, making it difficult to identify by eye. So, as a final test, we examine the total number of red clump stars in each of the ACS grids. Figure 10(a) shows the grid

4 Hess CMD with the red clump selection region overlaid; the same selection region is applied to the CMD and photometry of each grid. Recall that our photometry is complete to more than 2 magnitudes below the red clump; such a population is easily detectable in our data.

In Figure 10(b) we plot the number of red clump stars in each grid position as a function of distance from the dynamical center of NGC 6822 [ $19^{\text{h}}44^{\text{m}}58.04^{\text{s}}$ ,  $-14^{\circ}49'18.9''$  (J2000) from Weldrake et al. (2003)]. The number of red clump stars per unit area falls exponentially as a function of radius, with a scale length of 545 pc; this compares favorably with the scale length of 430 pc found by Letarte et al. (2002) using the carbon star population. The number density of red clump stars at the grid 1 position is well within the  $1\sigma$  error bar of the exponential fit. This plot is exactly what is expected for an exponentially declining surface brightness distribution as a function of radius. We therefore fail to detect evidence of an ancient stellar population that can be attributed to a bona fide low-mass companion object at this location. This is in agreement with the observation by Weldrake et al. (2003) that the velocity field in NGC 6822 is very highly symmetric in that the rotation curves derived from the approaching and receding sides are nearly identical. A true interaction would be expected to distort the velocity field in an observable manner. Given the high degree of symmetry, the most likely explanation for the HI morphology is a warp in which the outer HI is more highly inclined than the inner HI (in agreement with the tilted ring model results found by Weldrake et

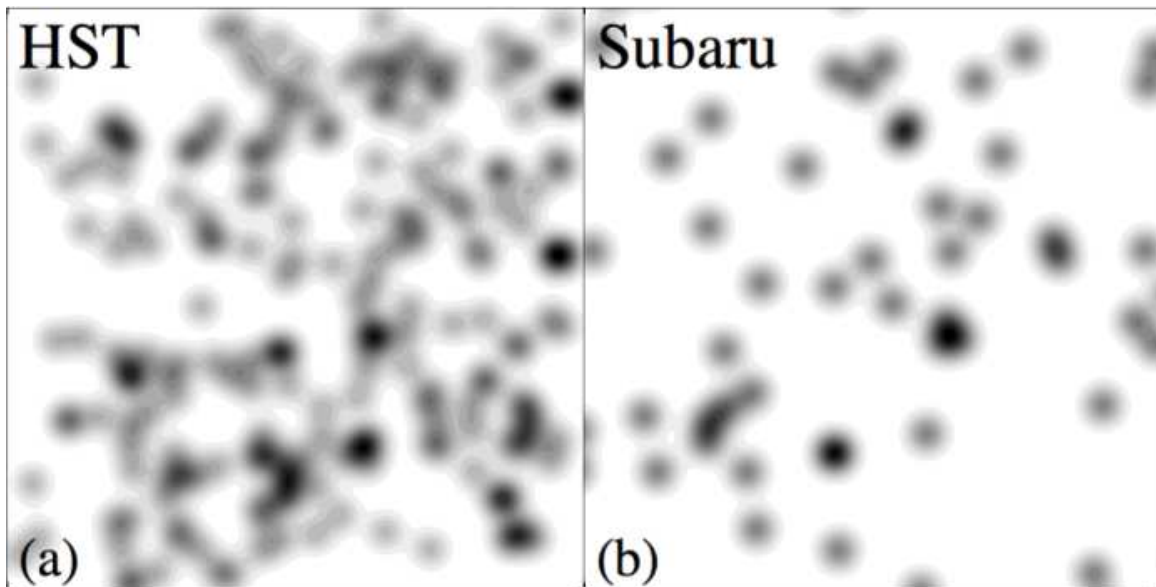


FIG. 9.— Smoothed distribution of red giant branch stars detected by both *HST* and by the combined *Subaru* dataset from de Blok & Walter (2006). In grid 1 we see no spatial concentration of red giant branch stars indicative of the companion.

al. 2003).

Taken as a whole, the evidence above challenges the hypothesis that the putative companion is a bona fide dwarf galaxy that harbors an ancient stellar population. The origin of the global SF event during the most recent  $\sim 50$  Myr (which varies in intensity from one grid position to another) may be caused by a gravitational interaction, but we do not find evidence that the object in the NW is the interacting partner. This event may simply be stochastic - a result of the small number of young blue stars required to increase the SFR by the observed amounts in the grids with weaker SFRs.

A powerful diagnostic of the nature of this putative companion would be an observed metallicity difference between it and the main stellar body. The coarse metallicities of each field derived by our SFH show no evidence for such an offset. This further weakens the companion hypothesis. Of course, direct abundance estimators would be preferable; in this regard, deep long-slit spectroscopy of the faint HII regions in the putative companion and/or of the red giant branch stars therein would be most useful in identifying any abundance difference between this object and the main stellar body.

## 5. ON THE ORIGIN OF THE SUPERGIANT HI HOLE

### 5.1. A Stellar Feedback Origin

The large hole in the neutral gas distribution of NGC 6822 has been enigmatic since its discovery (Gottesman & Weliachew 1977; Skillman 1992; Brandenburg & Skillman 1998; de Blok & Walter 2000). The size of the structure ( $\sim 2 \text{ kpc} \times 1.4 \text{ kpc}$ ), the lack of observed expansion, and the offset location with respect to the high surface brightness stellar distribution (see Figure 1) make it a particularly important test case for the hypothesis that stellar evolution can create such structures via coherent feedback. We now examine the recent SF within this structure with the particular goal of discerning if stellar feedback processes are capable of producing it.

The recent SFH of the HI hole field (grid 5; see Fig-

ures 6 and 7) is characterized by activity in the  $\sim 500$ -400 Myr and the most recent  $\sim 50$  Myr periods, with a period of relative inactivity between. Note that all of the SFRs are comparatively low; even at the height of activity, the SFR only reaches a level of order  $10^{-4} \text{ M}_{\odot} \text{ yr}^{-1}$ . Since the HI structure has no observed expansion velocity (and thus no empirical constraint on its age), we apply the methodology developed in Weisz et al. (2009a) to derive the amount of stellar feedback energy input into this region over the most recent 500 or 100 Myr periods. These calculations yield  $9.8 \times 10^{52}$  erg and  $1.2 \times 10^{52}$  erg for the most recent 500 Myr and 100 Myr intervals, respectively. Note that we make no correction for the contributions of Type Ia SNe to the feedback energy budget, as has been shown to be important (Recchi & Hensler 2006). These events occur over a range of timescales (Matteucci et al. 2006) and may occur in regions that are already partially evacuated. Thus, the feedback energies derived from stellar evolution should be considered lower limits.

The ability of this feedback energy to evacuate the surrounding material depends critically on how much energy is converted into gas motion. If one assumes a 100% conversion efficiency of feedback energy into the motion of the surrounding gas, then the feedback energy budget over the last 500 Myr reaches  $\sim 10^{53}$  erg, the value derived by de Blok & Walter (2000) using an adopted age of 100 Myr and the single-blast SN prescriptions in Chevalier (1974).

Note that the required blast energies estimated in this way are highly model dependent and thus highly uncertain (Warren et al. 2011). Additionally, we stress that assuming an efficiency of 100% is likely not physical and is much higher than most derived values found in nearby galaxies (e.g., Weisz et al. 2009b; Cannon et al. 2011b; Warren et al. 2011), as well as higher than predictions from numerical simulations (e.g., Theis et al. 1992; Cole et al. 1994; Padoan et al. 1997; Thornton et al. 1998). With a more realistic assumption of 20% efficiency, the timescale for the requisite feedback energy extends well past 500 Myr.

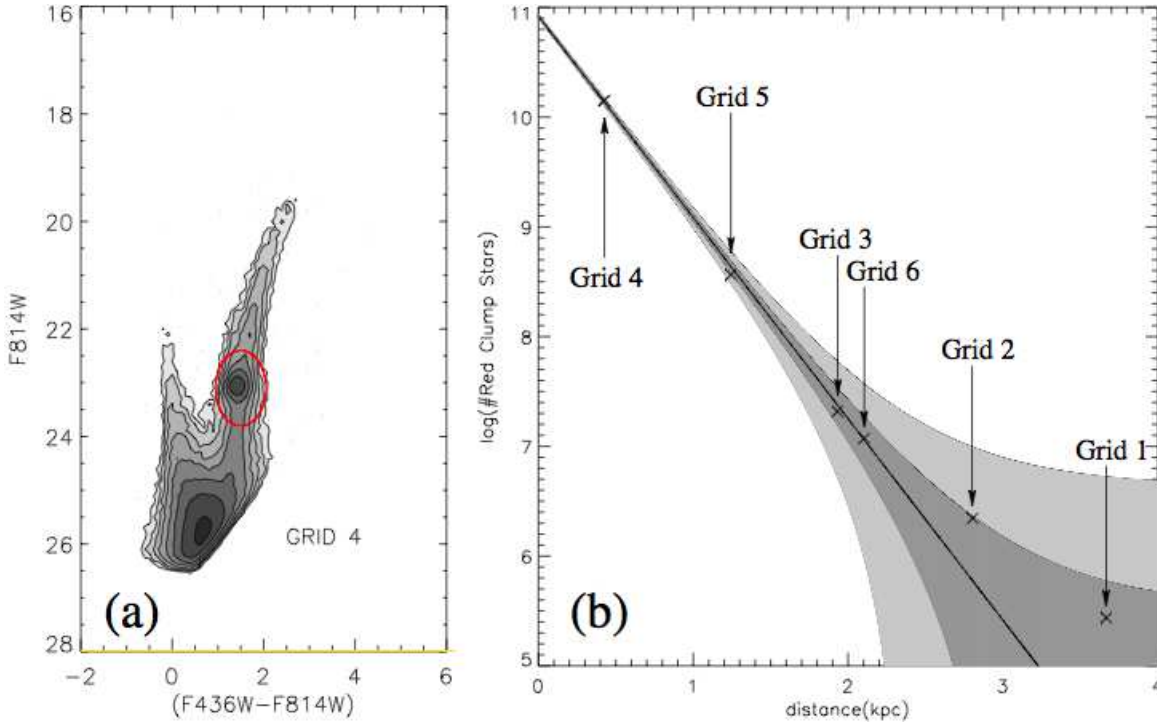


FIG. 10.— The number of red clump stars versus galactocentric radius. Panel (a) shows the grid 4 Hess diagram CMD (same as shown in Figure 4), with the red clump selection region overlaid in red; this same region is selected in each of the six ACS grids. Panel (b) shows a logarithmic plot of the number of red clump stars in each grid versus the projected distance from the dynamical center. The solid line is an exponential fit to the data points; the dark and light gray regions in (b) show the  $1\sigma$  and  $2\sigma$  bounds on this fit. In creating this plot we have adopted a dynamical center position of  $(\alpha, \delta) = (19^{\text{h}}44^{\text{m}}58.04^{\text{s}}, -14^{\circ}49'18.9'')$  (J2000) from Weldrake et al. (2003) and a distance of 492 kpc for the galaxy. We find no evidence for an over-density of ancient stars at the location of grid 1.

Despite the uncertainties, it is clear that the energy produced by stars in the last 100 Myr is unlikely to have been able to produce the HI hole. It is likely that the energy from star formation over at least the last 500 Myr is required to have produced the present HI hole. Assuming a stellar feedback origin, this implies that holes can persist for much longer than the dynamical timescale ( $\sim 140$  Myr; McQuinn et al. 2010). HI holes with dynamical ages of a few hundred Myr have been observed before (see, e.g., Weisz et al. 2009b; Cannon et al. 2011b; Warren et al. 2011), and have theoretical support from simulations (e.g., Recchi & Hensler 2006). Such long-lived structures might be considered to be more likely in the lower surface density outer HI disk of a system like NGC 6822 which is undergoing solid-body rotation, since there is no rotational shear to remove the structure. Indeed, the models of Mac Low & Ferrara (1999) show that the position with respect to the galactic midplane is an important parameter in the evolution of expanding structures that result from SF. We postulate that the typical HI hole in a low-mass galaxy is in fact long-lived, explaining, in part, the lack of observed expansion velocities for many of the holes and shells in nearby dwarfs (e.g. Bagetakos et al. 2011).

## 5.2. Alternative Creation Mechanisms

Could the HI hole have been caused by a gravitational interaction with the putative companion? In such a scenario, we would expect a global burst of SF in both the hole (grid 5) and the companion (grid 1) on a timescale compatible with the dynamical time. While we do see a weak SF signature within the most recent  $\sim 50$  Myr (al-

though the relative increases in SFRs are small in both grid positions), the current relative separation of the HI hole and the putative companion ( $\sim 34'$ ) would require a relative velocity of  $\sim 95 \text{ km s}^{-1}$  over this 50 Myr timescale in order for the events to be causally connected. Assuming that neutral gas was involved in this interaction, such a signature would be very obvious in the HI data and is inconsistent with the observed velocity structure presented in de Blok & Walter (2000) and Weldrake et al. (2003). When coupled with the lack of evidence for an ancient stellar population at the location of grid 1 (see § 4), we conclude that an interaction with the putative companion is an unlikely creation mechanism for the giant HI hole.

The interaction scenario remains promising, however, based on the morphology of the neutral gas alone. The extensions of the HI disk to the NW and SE could be indicative of tidal features that might arise during an interaction. The involvement of any other Local Group galaxy in such a potential interaction seems unlikely due to the galaxy's relative isolation. de Blok & Walter (2000) unsuccessfully searched a 10 square degree area around NGC 6822 for companions detected by HIPASS (Meyer et al. 2004). However, we note that NGC 6822 has a negative heliocentric velocity and thus is mildly confused with Galactic HI emission. Subsequent observations with the Parkes 64m multi-beam receiver (Weldrake et al. 2003) show that most of the Galactic emission can be separated from that within NGC 6822, although a small velocity range ( $\sim 10 \text{ km s}^{-1}$ ) centered in the SE region could contain moderate Galactic contamination. A small perturbing HI cloud thus remains

a viable, though unlikely, mechanism for the creation of the HI hole and the extended tidal structure of NGC 6822.

Various other creation mechanisms of the HI hole could be considered, although none is as successful in explaining the current properties of NGC 6822 as a stellar feedback origin. For example, ram pressure could preferentially remove the neutral gas from a low-density outer disk region (e.g., Bureau & Carignan 2002). While the size of the giant HI hole, and the lack of similar-scale structures elsewhere in the outer disk argue against ram pressure stripping as the sole creation mechanism for the giant HI hole, Bureau & Carignan (2002) argue that ram pressure has the capacity to enlarge pre-existing holes and lower their creation energies. This would help to “bridge the gap” between the observed star formation rate and that required to create the holes, thus resulting in lower creation ages.

Similarly, outflow or inflow of material from/to the disk of NGC 6822 could in principle give rise to this structure. The size and location of the HI structure argue strongly against the outflow scenario. Infall of material is more difficult to dismiss and could be considered tantamount to an interaction with a small gas cloud as mentioned above. Finally, recent simulations show that interactions between dark matter sub-halos and gaseous disks are unlikely creation mechanisms for HI holes and shells (Kannan et al. 2012); such a scenario in the NGC 6822 system is unlikely.

## 6. SUMMARY AND DISCUSSION

We have presented new *HST*/ACS imaging of six fields that span the HI major axis of the Local Group dwarf galaxy NGC 6822. These positions are selected in order to probe the stellar populations within the putative companion in the NW, the giant HI shell in the SE, and the extended tidal material in the outer disk of the galaxy. The photometry reaches two magnitudes below the red clump and is extremely sensitive to SF within the most recent 500 Myr in each of the grid positions.

Remarkably, the SFHs of the six grid locations are essentially identical to one another. While the relative SFRs change from one grid location to another, each of the six observed positions underwent a period of heightened SF activity in the most recent  $\sim 50$  Myr interval. This interval is shorter than the dynamical timescale of the system ( $\sim 140$  Myr) and argues for a galaxy-wide event at this time.

The cumulative ancient SFHs of the six grid positions are qualitatively similar, and reveal that NGC 6822 has formed half of its total stellar mass within the most recent  $\sim 5$  Gyr. This argues against the inside-out growth of the disk in this system, as seen in some other nearby galaxies. The similarity of the ancient cumulative SFH of the putative companion and the other observed regions suggests that this region is indistinguishable from the outer halo of NGC 6822.

This interpretation is strengthened by the lack of a coherent ancient stellar population at the location of grid 1. We find no over-density of red giant branch stars at the location of the putative companion, using either our new *HST* data or the previously published *Subaru* data (de Blok & Walter 2006). We capitalize on the photometric depth of our *HST* images to derive the number

of red clump stars in each of the six grid positions; the number of red clump stars per unit area falls off as a perfect exponential function as one moves into the outer disk, and the number of stars in grid 1 is well within the  $1\sigma$  error bound on this fit. We conclude that the putative companion is not a bona fide galaxy (i.e., one containing an ancient stellar population).

The stellar populations within the giant HI hole show a strong and well-populated red giant branch and red clump. While the blue plume is weak, there is nonetheless evidence for low-level SF activity over the last 500 Myr. Feedback from SF in the most recent 100 Myr is not energetic enough to produce the HI hole. Only when we integrate over a much longer time interval ( $>500$  Myr, i.e., significantly longer than the dynamical timescale) and assume a high feedback efficiency do we recover sufficient feedback energy to meet the  $\sim 10^{53}$  erg requirement derived by de Blok & Walter (2000).

The giant HI hole in NGC 6822 is an especially important test case for the hypothesis that stellar feedback can create such structures. We find evidence for extended star formation that gives rise to this structure. The timescale for this feedback exceeds the dynamical time of the galaxy. This adds further evidence for long-lived HI structures in solid-body rotating galaxies (see, e.g., Weisz et al. 2009b; Cannon et al. 2011b; Warren et al. 2011). We propose that long-lived holes and shells in the neutral ISM of dwarf galaxies are the norm; once formed they remain coherent for long periods of time. The lack of dynamical processes to remove these structures allows them to persist for hundreds of Myr in the outer disks of low-mass systems.

We consider various other creation mechanisms for the HI hole, in an attempt to explain the enigmatic properties of the NGC 6822 system; none is as successful as feedback from extended SF. The overall neutral gas morphology is indicative of a tidal interaction; the kinematic discontinuities identified near the position of the putative companion by de Blok & Walter (2000) support this interpretation. From our *HST* imaging we rule out the putative companion as being a bona fide galaxy that took part in this interaction. However, an interaction with a gas cloud without an ancient stellar component (e.g., a high velocity cloud analog) remains a viable solution; the confusion of NGC 6822 with Galactic HI may allow such a companion to remain hidden in the current datasets.

We are observing NGC 6822 at a unique time in its evolution. Numerous open questions about the evolution of low-mass galaxies can be addressed by further studies of this enigmatic object. Of particular value would be higher spatial and spectral resolution HI imaging of the entire gas disk, facilitating detailed kinematic modeling of the tidal arms, the putative companion, and the giant HI hole. Such data would help to differentiate between the companion hypothesis for the NE HI cloud and a more simplistic, non-uniform HI distribution with changing inclination angle as a function of galactocentric radius.

We thank the referee, Antonio Aparicio, for insightful comments that improved this manuscript. Partial support for this research was provided by NASA through grant GO-12180 from the Space Telescope Sci-

ence Institute, which is operated by AURA, INC., under NASA contract NAS5-26555. J.M.C. and E.M.O. thank Macalester College for research support. This investigation has made use of the NASA/IPAC Extragalactic

Database (NED) which is operated by the Jet Propulsion Laboratory, California Institute of Technology, under contract with the National Aeronautics and Space Administration, and NASA's Astrophysics Data System.

## REFERENCES

- Bagetakos, I., Brinks, E., Walter, F., et al. 2011, *AJ*, 141, 23
- Brandenburg, H. J., & Skillman, E. D. 1998, *Bulletin of the American Astronomical Society*, 30, 1354
- Bureau, M., & Carignan, C. 2002, *AJ*, 123, 1316
- Cannon, J. M., et al. 2011a, *ApJ*, 735, 35
- Cannon, J. M., et al. 2011b, *ApJ*, 735, 36
- Chevalier, R. A. 1974, *ApJ*, 188, 501
- Cole, S., Aragon-Salamanca, A., Frenk, C. S., Navarro, J. F., & Zepf, S. E. 1994, *MNRAS*, 271, 781
- Cole, A. A., et al. 2007, *ApJ*, 659, L17
- de Blok, W. J. G., & Walter, F. 2000, *ApJ*, 537, L95
- de Blok, W. J. G., & Walter, F. 2003, *MNRAS*, 341, L39
- de Blok, W. J. G., & Walter, F. 2006, *AJ*, 131, 343
- de Jong, J. T. A., Yanny, B., Rix, H.-W., et al. 2010, *ApJ*, 714, 663
- Dohm-Palmer, R. C., Skillman, E. D., Saha, A., et al. 1997, *AJ*, 114, 2527
- Dohm-Palmer, R. C., Skillman, E. D., Gallagher, J., et al. 1998, *AJ*, 116, 1227
- Dolphin, A. E. 2000, *PASP*, 112, 1383
- Dolphin, A. E. 2002, *MNRAS*, 332, 91
- Dolphin, A. E., Saha, A., Skillman, E. D., et al. 2003, *AJ*, 126, 187
- Dotter, A., Chaboyer, B., Jevremović, D., et al. 2008, *ApJS*, 178, 89
- Elmegreen, B. G., & Hunter, D. A. 2000, *ApJ*, 540, 814
- Fiorentino, G., et al. 2010, *ApJ*, 711, 808
- Ford, H. C., Bartko, F., Bely, P. Y., et al. 1998, *Proc. SPIE*, 3356, 234
- Gallagher, J. S., III, & Hunter, D. A. 1989, *AJ*, 98, 806
- Gallagher, J. S., Tolstoy, E., Dohm-Palmer, R. C., et al. 1998, *AJ*, 115, 1869
- Gallart, C., Zoccali, M., & Aparicio, A. 2005, *ARA&A*, 43, 387
- Girardi, L., Bertelli, G., Bressan, A., et al. 2002, *A&A*, 391, 195
- Girardi, L., Williams, B. F., Gilbert, K. M., et al. 2010, *ApJ*, 724, 1030
- Gottesman, S. T., & Weliachew, L. 1977, *A&A*, 61, 523
- Heckman, T. M., Armus, L., & Miley, G. K. 1990, *ApJS*, 74, 833
- Hidalgo, S. L., Marín-Franch, A., & Aparicio, A. 2003, *AJ*, 125, 1247
- Hidalgo, S. L., Aparicio, A., Martínez-Delgado, D., & Gallart, C. 2009, *ApJ*, 705, 704
- Hidalgo, S. L., et al. 2011, *ApJ*, 730, 14
- Hodge, P., Smith, T., Eskridge, P., MacGillivray, H., & Beard, S. 1991, *ApJ*, 379, 621
- Jarosik, N., Bennett, C. L., Dunkley, J., et al. 2011, *ApJS*, 192, 14
- Kannan, R., Maccio, A. V., Pasquali, A., Moster, B. P., & Walter, F. 2012, *ArXiv/1107.2401*
- Kroupa, P. 2001, *MNRAS*, 322, 231
- Lee, M. G., Freedman, W. L., & Madore, B. F. 1993, *ApJ*, 417, 553
- Letarte, B., Demers, S., Battinelli, P., & Kunkel, W. E. 2002, *AJ*, 123, 832
- Mac Low, M.-M., & Ferrara, A. 1999, *ApJ*, 513, 142
- Mateo, M. L. 1998, *ARA&A*, 36, 435
- Matteucci, F., Panagia, N., Pipino, A., Mannucci, F., Recchi, S., & Della Valle, M. 2006, *MNRAS*, 372, 265
- McQuinn, K. B. W., et al. 2010, *ApJ*, 724, 49
- Meyer, M. J., et al. 2004, *MNRAS*, 350, 1195
- Orban C., Gnedin O.Y., Weisz D.R., Skillman E.D., Dolphin A.E., & Holtzman J.A. 1998, *ApJ*, 686, 1030
- Östlin, G. 2000, *ApJ*, 535, L99
- Padoan, P., Jimenez, R., & Jones, B. 1997, *MNRAS*, 285, 711
- Putman, M. E., Gibson, B. K., Staveley-Smith, L., et al. 1998, *Nature*, 394, 752
- Recchi, S., & Hensler, G. 2006, *A&A*, 445, L39
- Skillman, E. D. 1992, *Elements and the Cosmos*, 246
- Tenorio-Tagle, G., & Bodenheimer, P. 1988, *ARA&A*, 26, 145
- Theis, C., Burkert, A., & Hensler, G. 1992, *A&A*, 265, 465
- Thornton, K., Gaudlitz, M., Janka, H.-T., & Steinmetz, M. 1998, *ApJ*, 500, 95
- Tolstoy, E., Gallagher, J. S., Cole, A. A., et al. 1998, *AJ*, 116, 1244
- Warren, S. R., Weisz, D. R., Skillman, E. D., et al. 2011, *ApJ*, 738, 10
- Weisz, D. R., Skillman, E. D., Cannon, J. M., Dolphin, A. E., Kennicutt, R. C., Jr., Lee, J., & Walter, F. 2008, *ApJ*, 689, 160
- Weisz, D. R., Skillman, E. D., Cannon, J. M., Walter, F., Brinks, E., Ott, J., & Dolphin, A. E. 2009a, *ApJ*, 691, L59
- Weisz, D. R., Skillman, E. D., Cannon, J. M., Dolphin, A. E., Kennicutt, R. C., Jr., Lee, J., & Walter, F. 2009b, *ApJ*, 704, 1538
- Weisz, D. R., et al. 2011, *ApJ*, 743, 8
- Weldrake, D. T. F., de Blok, W. J. G., & Walter, F. 2003, *MNRAS*, 340, 12
- Williams, B. F., Dalcanton, J. J., Dolphin, A. E., Holtzman, J., & Sarajedini, A. 2009, *ApJ*, 695, L15